Proceedings of HTC'03
ASME Summer Heat Transfer Conference
July 21-23, 2003, Las Vegas, Nevada, USA

HT2003-47051

REVIEW OF THERMAL JOINT RESISTANCE MODELS FOR NON-CONFORMING ROUGH SURFACES IN A VACUUM

Bahrami M.[1], **Culham J. R.**[2], **Yovanovich M. M.**[3] **and Schneider G. E.**[4]
Microelectronics Heat Transfer Laboratory,
Department of Mechanical Engineering,
University of Waterloo, Waterloo, Ontario, Canada

ABSTRACT

The thermal contact resistance (TCR) problem is categorized into three different problems: geometrical, mechanical, and thermal. Each problem includes a macro and micro scale subproblem; existing theories and models for each part are reviewed.

Empirical correlations for microhardness, and the equivalent (sum) rough surface approximation are discussed. Suggested correlations for estimating the mean absolute surface slope are summarized and compared with experimental data.

The classical conforming rough contact models, i.e elastic and plastic, as well as elastoplastic models are reviewed. A set of scale (dimensionless) relationships are derived for the contact parameters, i.e. the mean microcontact size, number of microcontacts, density of microcontacts, and the external load as functions of dimensionless separation, for the above models. These scale relationships are plotted; it is graphically shown that the behavior of these models, in terms of the contact parameters, are similar.

The most common assumptions of existing thermal analysis are summarized. As basic elements of thermal analysis, spreading resistance of a circular heat source on a half-space and flux tube are reviewed, also existing flux tube correlations are compared.

More than 400 TCR data points collected by different researchers during last forty years are grouped into two limiting cases: conforming rough, and elasto-constriction. Existing TCR models are reviewed and compared with the experimental data at these two limits. It is shown that the existing theoretical models do not cover both of the above-mentioned limiting cases.

NOMENCLATURE

A	=	area, m^2
a	=	radius of contact, m
b	=	flux tube radius, m
c_1, c_2	=	microhardness coefficients, $GPa, -$
d	=	mean plane separation, GW model
d_V	=	Vickers indentation diagonal, μm
E	=	Young's modulus, GPa
E'	=	equivalent elastic modulus, GPa
F	=	external force, N
H, H_B	=	bulk hardness, GPa
H_{mic}	=	microhardness, GPa
H_{BGM}	=	geometric mean Brinell hardness, GPa
h	=	thermal contact conductance, W/m^2K
k	=	thermal conductivity, W/mK
k_s	=	harmonic mean thermal conductivity, W/mK
L	=	sampling length, m
m	=	effective mean absolute surface slope, $-$
m'	=	effective RMS surface slope, $-$
n_s	=	number of microcontacts
P	=	pressure, Pa
Q	=	heat flow rate, W
q	=	heat flux, W/m^2
R	=	thermal contact resistance, K/W
RMS	=	root mean square
R_a	=	arithmetic average surface roughness, μm
R_q	=	RMS surface roughness, μm
T	=	temperature, K
Y	=	mean surface plane separation, m

[1]Ph.D. Candidate, Department of Mechanical Engineering.
[2]Associate Professor, Director, Microelectronics Heat Transfer Laboratory. member ASME .
[3]Distinguished Professor Emeritus, Department of Mechanical Engineering. Fellow ASME.
[4]Professor, Department of Mechanical Engineering.

Greek

β	=	summits radii of curvature, m
γ	=	plasticity index
δ	=	surface max out-of-flatness, m
ε	=	flux tube relative radius
η	=	microcontact density
κ	=	H_B/H_{BGM}
λ	=	dimensonless separation
ν	=	Poisson's ratio
ϕ	=	normal probability function
ψ	=	dimensionless spreading resistance
ρ	=	radius of curvature, m
σ	=	RMS surface roughness, μm
ω	=	normal deformation, m
ξ	=	emprical correction factor

Subscripts

0	=	value at origin
$1, 2$	=	surface 1, 2
a	=	apparent
b	=	bulk
c	=	conduction, contact
e	=	effective
g	=	gap
GW	=	Greenwood and Williamson
Hz	=	Hertz
j	=	joint
L	=	large (macro scale)
m	=	mean
mac	=	macro
mic	=	micro
r	=	real
s	=	small
V	=	Vickers

INTRODUCTION

Heat transfer through interfaces formed by the mechanical contact of two non-conforming rough solids, occurs in a wide range of applications, such as: microelectronic cooling, spacecraft structures, satellite bolted joints, nuclear engineering, ball bearings, and heat exchangers. Analytical, experimental, and numerical models have been developed to predict thermal contact resistance since the 1930's. The number of publications on thermal contact resistance amounts to several hundred papers, which illustrates the importance of this issue, and also indicates that the development of a general predictive model is a difficult task. Generally, contact between two surfaces occurs only over microscopic contacts. The real area of contact, the total area of all microcontacts, is typically a small fraction of the nominal contact area [1,2]. As illustrated in Fig.1, the macroscopic contact region arises due to out-of-flatness of bodies; and the microcontacts form due to interface between contacting asperities of rough surfaces. In these situations heat flow experiences two stages of resistance in series, macroscopic and microscopic constriction resistance [3-5]. This phenomenon leads to a relatively high temperature drop across the interface.

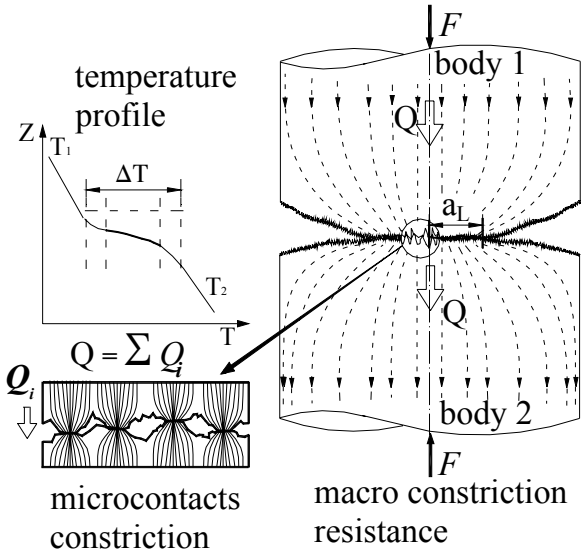

Figure 1. Macro and micro thermal constriction/spreading resistances

Thermal energy can be transferred between contacting bodies by three different modes, i) conduction at the microcontact spot, ii) conduction through the interstitial fluid in the gap between the contacting solids, and iii) thermal radiation across the gap. The radiation heat transfer remains small and can be neglected for surface temperatures up to 700 K [3,6]. Since in this study the interstitial fluid is assumed to be absent, the only remaining heat transfer mode is conduction at the microcontacts.

Thermal contact resistance (TCR) problems basically consist of three different problems: geometrical, mechanical, and thermal. Figure 2 illustrates the thermal contact resistance problem flow diagram and its components. The heart of a TCR analysis is its mechanical part. Any solution for the mechanical problem requires that the geometry of the contacting surfaces (macro and micro) be quantitatively described. The mechanical problem also includes two parts: macro or large-scale contact and micro or small-scale contact. The mechanical analysis determines the macrocontact radius, a_L, and the pressure distribution for the large-scale problem. For the microcontact problem separa-

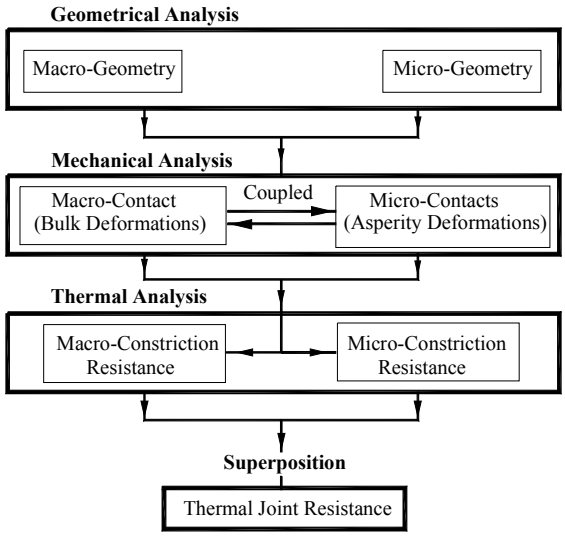

Figure 2. Thermal contact resistance modeling flow diagram

tion between the mean contacting planes, microcontact size, density of microcontacts, and the relative microcontact radius are calculated. The macro and the micro mechanical problems are coupled. The thermal analysis, based on the results of the mechanical analysis, is then used to calculate the microscopic and macroscopic thermal resistances.

GEOMETRICAL ANALYSIS

It is necessary to consider the effect of both surface roughness and out-of-flatness on the contact of nonconforming rough surfaces. Therefore, the geometrical analysis is divided into micro and macro parts.

Micro Geometrical Analysis

All solid surfaces are rough, this roughness or surface texture, can be thought of as the surface deviation from the nominal topography. Surface textures can be created using many different processes. Most man-made surfaces, such as those produced by grinding or machining have a pronounced "lay". Generally, the "Gaussian surface" term is used to refer to a surface, where its asperities are isotropic and randomly distributed over the surface. It is not easy to produce a wholly isotropic roughness. The usual procedure for experimental purposes is to air-blast a metal surface with a cloud of fine particles, in the manner of shot peening, which gives rise to a randomly created surface. According to Liu, et al. [8] five types of instruments are currently available for measuring the surface topography, namely: stylus-type surface profilometer, optical (white-light interference) measurements, Scanning Electron Microscope (SEM), Atomic Force Microscope (AFM), and Scanning Tunneling Microscope (STM). Among these, the first two instruments are usually used for macro-to-macro asperity measurements, whereas the others may be used for micro or nanometric measurements. Surface texture is most commonly measured by a profilometer, which draws a stylus over a sample length of the surface. A datum or centerline is established by finding the straight line (or circular arc in the case of round components) from which the mean square deviation is a minimum. The arithmetic average of the absolute values of the measured profile height deviations, R_a, taken within a sampling length from the graphical centerline [9]. The value of R_a is

$$R_a = \frac{1}{L}\int_0^L |z(x)|\,dx \tag{1}$$

where, L is the sampling length in the x direction and z is the measured value of the surface height along this length. When the surface is Gaussian, the standard deviation σ is identical to the RMS value, R_q

$$\sigma = R_q = \sqrt{\frac{1}{L}\int_0^L z^2(x)\,dx} \tag{2}$$

For a Gaussian surface, Ling [10] showed that the average and RMS heights are related as follows

$$R_q \approx \sqrt{\frac{\pi}{2}} R_a \approx 1.25 R_a \tag{3}$$

Similarly, the absolute average and RMS asperity slopes, m and m' respectively, can be determined across the sampling length from the following

$$m = \frac{1}{L}\int_0^L \left|\frac{dz(x)}{dx}\right| dx,\ m' = \sqrt{\frac{1}{L}\int_0^L \left(\frac{dz(x)}{dx}\right)^2 dx} \tag{4}$$

Mikic and Rohsenow [4] showed that for Gaussian surfaces the relationship between the average and RMS values of the asperity slopes is $m' \approx 1.25m$. Tanner and Fahoum [11] and Antonetti et al. [12], using published experimental surface data, suggested empirical correlations to relate RMS asperity slope, m', to average roughness, R_a. Lambert [13], also

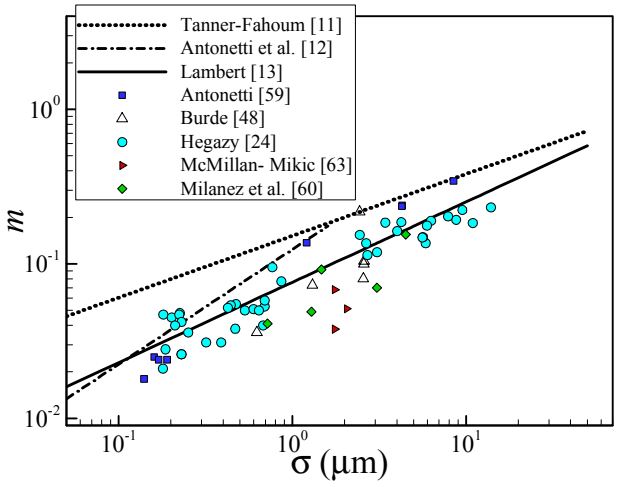

Figure 3. Comparison between correlations for m and experimental data

Table 1. Correlations for m, Gaussian surface

Reference	Correlation
Tanner and Fahoum [11]	$m = 0.152\ \sigma^{0.4}$
Antonetti et al. [12]	$m = 0.124\ \sigma^{0.743}, \quad \sigma \leq 1.6\,(\mu m)$
Lambert [13]	$m = 0.076\ \sigma^{0.52}$

using the same method, correlated the absolute average asperity slopes, m, as a function of RMS roughness (micron); correlations for m are summarized in Table 1. Figure 3 illustrates the comparison between these correlations and experimental data. As shown in Fig.3, the uncertainty of the above correlations is high, and use of these correlations are justifiable only where the surface slope is not reported and or a rough estimation of m is needed.

Equivalent (Sum) Rough Surface According to the examination of the microgeometry with equivalent magnitude in the vertical direction and in the traversing direction, asperities seem to have curved shapes at their tops [14]. A common assumption/methodology to model the surface roughness is the representation of surface asperities by simple geometrical shapes with a probability distribution for the different asperity parameters involved. One of the first presentations to use this asperity-based model is found in Coulomb's work in 1782. To explain the laws of friction, he assumed that the asperities possessed a spherical shape all of which had the same radius and the same summit altitude. Greenwood and Williamson [1] assumed that each asperity summit had a spherical shape whose height above a reference plane had a normal (Gaussian) probability density function. Williamson et al. [15] have shown experimentally that many of the techniques used to produce engineering surfaces give a Gaussian distribution of surface heights.

The solution of any contact mechanics problem requires that the geometry of the intersection and overlap of the two undeformed surfaces be known as a function of their relative position. Greenwood [16] stated that; "*a genuine treatment of two rough surfaces is complicated by the difficulty of describing the unit event, the formation of a single contact spot. For example, if both surfaces are covered by spheres, it is necessary to study the contact of one sphere on the shoulder of another, and then evaluate the probabilities of different degrees of misalignment, in order to get the average unit event. A non-genuine treatment is comparatively simple: both surfaces are taken to be rough with normal distributions. The statistical treatment now concerns the probability of the sum of two heights (which is also normally distributed) exceeding the separation, and this is exactly equivalent to a distribution of a single variable.*" In other words, the contact between Gaussian rough surfaces can be considered as the contact between a single Gaussian surface, having the effective (sum) surface characteristics, placed in contact with a perfectly smooth flat surface. Also, since the slope, m, of a profile is proportional to the difference between adjacent equispaced ordinates; m is Gaussian if the profile is Gaussian [17]. This simplification was used by many researchers, such as: Clausing and Chao [3], Cooper et al. [18], Francis [19], and Johnson [7]. The equivalent roughness and surface slope can be calculated from

$$\sigma = \sqrt{\sigma_1^2 + \sigma_2^2} \quad \text{and} \quad m = \sqrt{m_1^2 + m_2^2} \tag{5}$$

According to Francis [19], a contact model based on the sum (equivalent) surface circumvents the problem of misalignment of contacting peaks; in addition, the sum surface sees peak to valley and peak to saddle contacts. The sum surface of two Gaussian surfaces is itself Gaussian and if parent surfaces are not exactly Gaussian, the sum (equivalent) surface will be closer to Gaussian than the parent surfaces. Additionally, the sum surface will be in general less anisotropic than the two contacting surfaces, thus the Gaussian sum surface is a reasonable basis for a general contact model [19]. Figure 4 shows a normal section through the contact in which the surfaces are imagined to overlap without deforming, and the equivalent rough or sum surface of the contact in the same normal section. The overlap geometry as a function of the mean separation, Y, of the undeformed surfaces is thus given directly and exactly by the shape of the equivalent rough surface. The number of

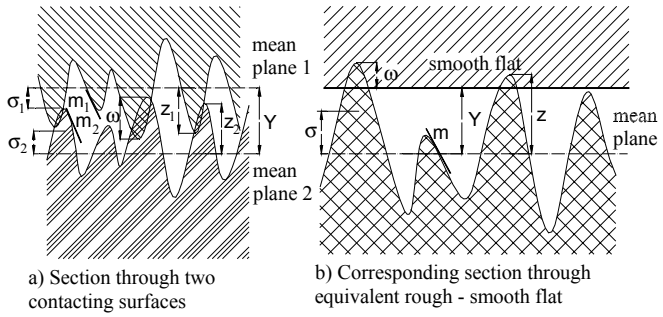

Figure 4. Equivalent contact of conforming rough surfaces

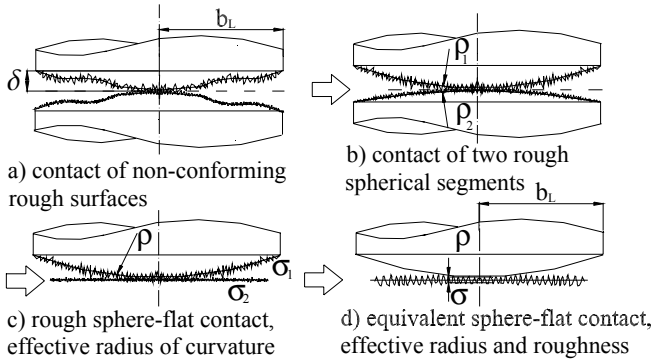

Figure 5. Flow diagram of geometrical modeling

microcontacts, which have formed, is simply the number of equivalent surface peaks that have; $Z \geq Y$.

Macro Geometrical Analysis

Many studies on thermal contact resistance ideally assume a uniform distribution of micro contact spots, i.e. conforming rough surface models. Such approaches are successful, where the macroscopic nonuniformity of the contact is negligible. However, no real engineering surfaces are perfectly flat, thus the influence of macroscopic nonuniformity can never be ignored. Considering the waviness or out-of-flatness of contacting surfaces in a comprehensive manner is very complex because of the case-by-case nature of the waviness. Certain simplifications must be introduced to describe the macroscopic topography of surfaces by a few parameters. A sphere is the simplest example of a macroscopically homogenous surface. Specifically, its profile is described only by its radius. Theoretical approaches by Clausing and Chao [20], Mikic and Rohsenow [4], Yovanovich [5], Nishino et al. [21], and Lambert and Fletcher [22] assumed that a spherical profile may approximate the shape of the macroscopic nonuniformity. According to Lambert [13] this assumption is justifiable, because nominally flat engineering surfaces are often spherical, or crowned (convex) with a monotonic curvature in at least one direction.

According to Johnson [7], in static frictionless contact of solids, the contact stresses depend only upon the relative profile of the two surfaces, i.e. upon the shape of the interstitial gap between them before loading. The actual system geometry may be replaced, without loss of generality, by a flat surface and a profile, which results in the same undeformed gap between the surfaces. For convenience, all elastic deformations can be considered to occur in one body, which has an effective elastic modulus and the other body is assumed to be rigid. The effective elastic modulus can be found from

$$\frac{1}{E'} = \frac{1-\upsilon_1^2}{E_1} + \frac{1-\upsilon_2^2}{E_2} \tag{6}$$

where, E and υ are the Young's modulus and Poisson's ratio, respectively. For the contact of two spheres, the effective radius of curvature is:

$$\frac{1}{\rho} = \frac{1}{\rho_1} + \frac{1}{\rho_2} \tag{7}$$

The relation between radius of curvature and the maximum out-of-flatness is [3]

$$\rho = \frac{b_L^2}{2\delta} \tag{8}$$

where, δ is the maximum out-of-flatness of the surface.

Figure 5 details the procedure, which has been used widely for the geometric modeling of the actual contact between two curved rough bodies. As the result of the above, the complex geometry of non-conforming rough contacts can be simplified to the contact of the equivalent truncated spherical surface with the equivalent rough flat.

Microhardness

Hardness is defined as the resistance to permanent deformation; hardness definitions and tests can be found in various standard textbooks e.g. Tabor [2], and Mott [23]. The most common hardness testing method is the static indentation. In a static indentation test, a steady load

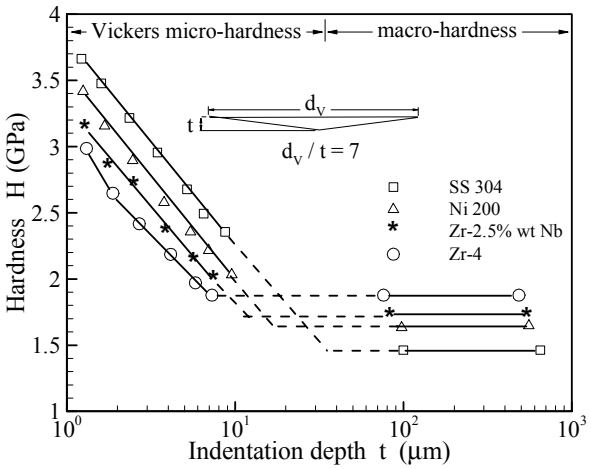

Figure 6. Measured hardness and microhardness, Hegazy [24]

is applied to an indenter which may be a ball, cone or pyramid and the hardness is calculated from the area or depth of indentation produced. Hegazy [24] demonstrated through experiments with four alloys, SS 304, nickel 200, zirconium-2.5% niobium, and Zircaloy-4, that the effective microhardness is significantly greater than the bulk hardness. As shown in Fig.6, microhardness decreases with increasing depth of the indenter until bulk hardness is obtained. Hegazy concluded that this increase in the plastic yield stress (microhardness) of the metals near the free surface is a result of local extreme work hardening or some surface strengthening mechanism. He derived empirical correlations to account for the decrease in contact microhardness of the softer surface with increasing depth of penetration of asperities on the harder surface

$$H_v = c_1 \left(d'_v\right)^{c_2} \tag{9}$$

where, H_v is Vickers microhardness in (GPa), $d'_v = d_v/d_0$ and $d_0 = 1\,(\mu m)$, d_v is Vickers indentation diagonal in (μm), and c_1, c_2 are correlation coefficients determined from experimental measurements. Table 2 shows c_1 and c_2 for some materials. Relating the hardness of a microcontact to the mean size of microcontacts, Hegazy [24] suggested a correlation for effective microhardness (conforming rough surfaces)

$$H_{mic} = c_1 \left(0.95 \frac{\sigma'}{m}\right)^{c_2} \tag{10}$$

where, $\sigma' = \sigma/\sigma_0$ and $\sigma_0 = 1\,(\mu m)$, σ is surface roughness in micrometers. Microhardness depends on several parameters: mean surface roughness, mean absolute slope of asperities, method of surface preparation, and applied pressure. Song and Yovanovich [25] related H_{mic} to the surface parameters and nominal pressure (conforming rough surface)

Table 2. Vickers microhardness coefficients, Hegazy [24]

Material	$c_1(GPa)$	c_2
Zr-4	5.677	-0.278
Zr-2.5wt% Nb	5.884	-0.267
Ni 200	6.304	-0.264
SS 304	6.271	-0.229

$$\frac{P}{H_{mic}} = \left[\frac{P}{c_1 \left(1.62\sigma'/m\right)^{c_2}}\right]^{1/(1+0.071c_2)} \tag{11}$$

Sridhar [26] suggested empirical relations to estimate Vickers microhardness coefficients, using the bulk hardness of the material. Two least-square-cubic fit expressions were reported

$$\begin{aligned} c_1 &= H_{BGM}\left(4.0 - 5.77\kappa + 4.0\kappa^2 - 0.61\kappa^3\right) \\ c_2 &= -0.57 + 0.82\kappa - 0.41\kappa^2 + 0.06\kappa^3 \end{aligned} \tag{12}$$

where, $\kappa = H_B/H_{BGM}$, H_B is the Brinell hardness of the bulk material, and $H_{BGM} = 3.178(GPa)$. The above correlations are valid for the range $1.3 \le H_B \le 7.6\ (GPa)$ with the RMS percent difference between data and calculated values were reported; 5.3% and 20.8% for c_1, and c_2, respectively.

MECHANICAL ANALYSIS

Figure 7 illustrates the mechanical analysis overview for contact of spherical rough surfaces, which includes; a macro and a micro part. Existing theories/models for each part (macro and micro) is categorized based on the normal deformation mode of the bulk (substrate) and asperities into: elastic, plastic, and elastoplastic groups.

Macrocontact Problem

When two smooth solid spheres, or equivalently a flat and the effective sphere, are pressed against each other, with increase in external load, the three ranges of loading: purely elastic, elastic-plastic (contained) and fully plastic (uncontained) occur in the most engineering structures. Hertz

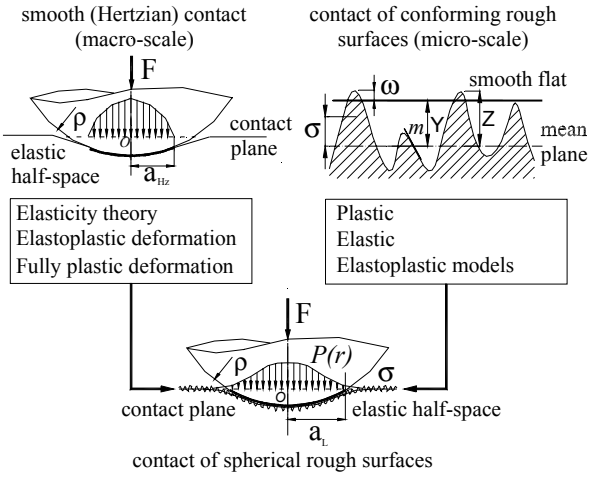

Figure 7. Mechanical problem overview for spherical rough contacts

[27] developed his elastic contact theory by introducing the simplification that each body can be regarded as an elastic half-space loaded over a small contact region of its plane surface. He also assumed surfaces are continuous and non-conforming, strains are small (to be in the elastic limit), surfaces are frictionless, and the pressure distribution is $P(r) = P_0\sqrt{1-(r/a_{Hz})^2}$. The Hertz theory expressions, can be summarized as

$$\begin{aligned} a_{Hz} &= \left(\frac{3F\rho}{4E'}\right)^{1/3} \\ \omega_0 &= \frac{a_{Hz}^2}{\rho} = \left(\frac{9F^2}{16\rho E'^2}\right)^{1/3} \\ P_0 &= \frac{3F}{2\pi a_{Hz}^2} = \left(\frac{6FE'^2}{\pi^3\rho^2}\right)^{1/3} \end{aligned} \tag{13}$$

where, ω_0 is the maximum deformation, and P_0 is the maximum pressure (at the center of the contact).

According to Johnson [7], the load at which plastic yield begins in the contact of two solids, is related to the yield point of the softer material. The yield point can be found either from Tresca's maximum shear stress, or Von Mises' shear strain-energy criterion. When the yield point is first exceeded the plastic zone is small and fully contained by material which remains elastic so that the plastic strains are of the same order of magnitude as the surrounding elastic strains. In these circumstances the material displaced by the indenter, is accommodated by an elastic expansion of the surrounding solid. As the indentation becomes more severe, the plastic zone (core) expands, and an increasing pressure is required beneath the indenter to produce the necessary expansion. Eventually the plastic zone breaks out to the free surface and displaced material is free to escape by plastic flow to the sides of the indenter. This is the uncontained mode of deformation, which should be analyzed by the theory of rigid-plastic solids [7]. However, the contact load must be increased about 400 times from the point of initial yielding to the state of fully plastic flow, which indicates that the elastoplastic transitional region is very long.

When the plastic deformation is severe so that the plastic strains are large compared with the elastic strains, the elastic deformation may be neglected. Provided the material does not strain-harden to a large extent, it may be idealized as a perfectly plastic solid, which flows plastically at a constant stress (roughly three times the yield stress) [7]. A loaded body of rigid-plastic material consists of regions in which, plastic flow takes place and regions in where there is no deformation due to the assumption of rigidity. Hardy et al. [28], using a numerical analysis, showed that the plastic flow leads to a flattening of the pressure distribution and at high loads may peak slightly towards the edge of the contact area.

Microcontact Problem

Based on the assumed deformation mode of asperities, existing microcontact mechanical models can be categorized into three main groups: plastic, elastic, and elastoplastic models. The fundamental assumptions, which are common in most of the models can be summarized as

- contacting surfaces are rough, isotropic, with a Gaussian asperity distribution
- behavior of a given microcontact is independent of all other microcontacts
- interfacial force on any microcontact spot acts normally (no friction)
- the deformation mechanics (i.e. the stress and displacement fields) are uniquely determined by the shape of the equivalent surface.

Plastic Models Abott and Firestone [29] developed the most widely used model for a fully plastic contact. With the concept of equivalent roughness, the model assumes that the asperities are flattened or, equivalently penetrate into the smooth surface without any change in the shape of the part of surfaces not yet in contact. Therefore, bringing the two surfaces together within a distance Y is equivalent to slicing off the top of the asperities at a height Y above the mean plane. Since the true area of contact is much smaller than

the apparent contact area, the pressure at the top of the asperities must be sufficiently large that they are comparable with the strength of the materials of the contacting bodies. Bowden and Tabor [30], and Holm [31] suggested that these contact pressures are equal to the flow pressure of the softer of the two contacting materials and the normal load is then supported by plastic flow of its asperities. Therefore, pressure at microcontacts will be equal to the microhardness and effectively independent of load and the contact geometry. The true area of contact is then proportional to the load, $A_r/A_a = P_m/H_{mic}$, where P_m is the mean apparent contact pressure.

Pullen and Williamson [32] experimentally investigated plastic flow under large loads. They assumed that material displaced from the contacting regions must reappear by raising some part of the non-contacting surface. They assumed that the volume of material remained constant and that the material that is plastically displaced appears as a uniform rise over the entire surface. Since the uniform rise will not affect the shape of the surface outside the contact area, they showed that the contact area due to the interaction of micro contacts is not proportional to the normal load (at relatively high loads); and proposed as a good approximation; $A_r/A_a = P_p/(1+P_p)$, where $P_p = P_m/H_{mic}$. Note that this phenomenon is important only at relatively large pressures.

Some authors used conical or curved shapes to describe the morphology of asperities. Tsukizoe and Kisakado [33,34], assumed a conical shape for surface asperities of equal base angle, which depends on the surface mean absolute slope. They proposed a statistical contact model for predicting the contact spot size and density for an isotropic Gaussian rough surface in contact with an ideal smooth flat surface. On the basis of this assumption and neglecting the asperity interactions, they obtained the following expressions for microcontact size and number

$$\begin{aligned} a_s &= \tfrac{\sqrt{2}}{\pi}(\sigma/m)/\lambda \\ n_s &= \tfrac{\sqrt{\pi}}{8}\left(\tfrac{m}{\sigma}\right)^2 \lambda \exp\left(-\lambda^2\right) A_a \end{aligned} \tag{14}$$

where, $\lambda = Y/\sqrt{2}\sigma$ is the dimensionless separation.

Cooper et al.[18], based on the level-crossing theory and using the sum surface approximation, derived relationships for mean microcontact size, and number of microcontacts by assuming hemispherical asperities whose height and surface slopes have Gaussian distributions

$$\begin{aligned} a_s &= \sqrt{\tfrac{8}{\pi}}(\sigma/m)\exp\left(\lambda^2\right)\operatorname{erfc}(\lambda) \\ n_s &= \tfrac{1}{16}A_a(m/\sigma)^2\exp\left(-2\lambda^2\right)/\operatorname{erfc}(\lambda) \end{aligned} \tag{15}$$

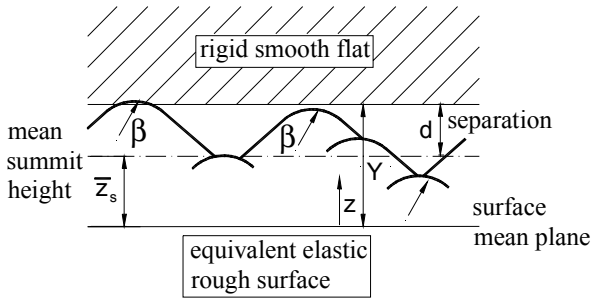

Figure 8. Greenwood and Williamson [1] geometrical model

Their model was essentially based on the assumption that each microcontact consists of two hemispherical asperities in symmetric (plastic) contact. They also showed that the ratio of real area of contact to the apparent area, as a function of Y, could be related to the probability function

$$\frac{A_r}{A_a} = \int_Y^\infty \phi(z)\,dz = \frac{1}{2}\operatorname{erfc}(\lambda) \tag{16}$$

where, $\phi(z)$ is the normal probability function of the asperity heights defined as

$$\phi(z) = \frac{1}{\sqrt{2\pi}\sigma}\exp\left(\frac{-z^2}{2\sigma^2}\right) \tag{17}$$

Elastic Models For applications such as lubrication or moving machine parts in which the contacting surfaces meet many times, Archard [35] pointed out that the asperities may flow plastically at first but they must reach a steady state in which the load is supported elastically. He then offered a model in which each asperity is covered with micro asperities, and each micro asperity with micro-micro asperities that gave successive closer approximations to the friction law, $A_r = F$, as more stages were considered.

Greenwood and Williamson [1] (GW) developed an elastic model for contact of flat rough surfaces based on the deformation of an average size summit. As shown in Fig.8, they assumed that all summits have the same radius of curvature at their top, and possess a Gaussian distribution about a mean reference plane, and the distribution of summit heights is the same as the heights standard deviation, i.e.: $\sigma_{\text{summit}} = \sigma$. GW model required three input

parameters: the standard deviation of summit height distribution σ_{summit}, the surface density of asperities η_{GW}, and the radius of curvature of the summits β that was assumed to be constant. Relationships for the GW model, as reported, are

$$\begin{aligned} n_s &= \eta_{GW} A_a I_0 (d') \\ A_r &= \pi \eta_{GW} A_a \beta \sigma I_1 (d') \\ F &= \frac{4}{3} \eta_{GW} A_a \beta^{1/2} \sigma^{3/2} E' I_{3/2} (d') \end{aligned} \tag{18}$$

where, $d' = d/\sigma$, and;

$$I_n (d') = \frac{1}{\sqrt{2\pi}} \int_{d'}^{\infty} (s - d')^n \exp\left(-s^2/2\right) ds \tag{19}$$

Unlike other models, the GW model is based on the contact of summits and separation, d, is measured from the mean summit line (not the surface mean line), which is located somewhere above the mean surface plane. Since it was assumed that the summits standard deviation is the same as the surface roughness, the GW relationships can be re-written as functions of $\lambda = Y/\sqrt{2}\sigma$ (to make the relationships comparable with other models). After evaluating the integrals and simplifying, the relationships become

$$\begin{aligned} n_s &= \frac{1}{2} \eta_{GW} A_a \text{erfc} (\lambda) \\ A_r &= \frac{\sqrt{\pi}}{2} \eta_{GW} A_a \beta \sigma \left[\exp\left(-\lambda^2\right) - \sqrt{\pi}\lambda \text{ erfc} (\lambda)\right] \\ F &= \frac{2^{1/4}}{3\sqrt{\pi}} \eta_{GW} A_a E' \beta^{1/2} \sigma^{3/2} \sqrt{\lambda} \exp\left(-\lambda^2/\ 2\right) \\ &\left[\left(1 + 2\lambda^2\right) K_{\frac{1}{4}} \left(\lambda^2/\ 2\right) - 2\lambda^2 K_{\frac{3}{4}} \left(\lambda^2/\ 2\right)\right] \end{aligned} \tag{20}$$

where, $K_n (.)$ is the modified Bessel function of the second kind of the nth order.

The GW asperity model has been extended to include other contact geometries, e.g. curved surfaces [36], more complex geometries, e.g. non-uniform radii of curvature of asperity peaks [37], and anisotropic surfaces [38]. Whitehouse and Archard [37] and Onions and Archard [39] further improved the statistic model by representing the features of the surface topography with two parameters: the standard deviation, σ, and the exponent of an exponential correlation function, which was named the "correlation distance". Bush et al. [40] developed an elastic contact model for isotropic surfaces that treated the asperities as elliptical paraboloids with random principal axis orientation and aspect ratio. O'Callaghan and Cameron [41] developed a model for the isotropic problem addressed by Bush et al. [40]. In their model, both surfaces can be rough and asperities need not contact at their tops. O'Callaghan and Cameron [41] concluded, as did Francis [19], that the contact of two rough surfaces was negligibly different from the contact of a smooth and an equivalent rough surface. McCool [42] compared the basic GW model with other more general isotropic and anisotropic models and found that the simpler GW model, despite its simplistic form, gives good results.

Elastoplastic Models Chang et al. [43], using GW model assumptions, presented a model based on volume conservation of an asperity control volume during plastic deformation. The deformed asperity was modeled as a truncated spherical segment and its radius was assumed to be the same as that of the undeformed asperity. For all plastically deformed asperities the average pressure over the contact area was assumed to be a factor of hardness, which was constant throughout the elastic-plastic deformation. Zhao et al. [44], using the Chang et al. [43] model, developed an elastic-plastic microcontact model for nominally flat rough surfaces. The transition from elastic deformation to fully plastic flow of the contacting asperities was curve-fitted. A cubic polynomial, smoothly joining the expressions for elastic and plastic area of contacts spans the elastoplastic region based on two extremes of the Chang et al. [43] model.

The advantage of the GW-type models is their (relative) simplicity and explicitness in expressions. However, assuming a constant summit radius is unrealistic; for a random surface, β is also a random variable [19]. In addition β and η_{GW} cannot be measured directly and must be calculated through statistical relationships, and are sensitive to the sampling length of the surface measurement [7].

Deformation Mode of Asperities When real surfaces are pressed together they make contact at numerous points, which deform, elastically, plastically or elastoplastically to support the load. According to Tabor [2] when two metals are placed in contact "*they will be supported on the tips of their asperities, at first the deformation is elastic, but for asperities of the order of μm radius, the minutest loads will produce plastic deformation. Indeed full plasticity may occur even for the hardest steels at a load of the order of a few milligrams.*" Tabor showed that in most practical cases, the real area of contact is proportional to the applied load. It is also inversely proportional to the effective hardness of the surface asperities. Greenwood [16] described the contact of two surfaces as: "*surfaces touch at a large number of contacts, and these contacts will be in all the states from fully*

elastic, to fully plastic. The fully elastic ones are a negligible fraction of the total; the effective flow pressure will be intermediate between plastic and elastic values." Considering the fact that the plastic flow is irreversible and cannot be repeated on subsequent loadings, Archard [35] emphasized the point that the normal contact must be elastic. He showed that any elastic model (based on simple Hertzian theory) in which the number of contacts remains constant will give $A_r \sim F^{2/3}$, which does not satisfy the observed proportionality $A_r \sim F$ reported by Tabor [2]. But, if the average contact size remains constant, and the number of microcontact increases, the area will be proportional to the load.

Greenwood and Williamson [1] introduced a plasticity index as a criterion for plastic flow of microcontacts, $\gamma_{GW} = (E'/H)\sqrt{\sigma/\beta}$. They reported that the load has little effect on the deformation regime. When the index is less than 0.6, plastic contact could be caused only if the surfaces were forced together under very large nominal pressure. When $\gamma_{GW} \geq 1$ plastic flow will occur even at small nominal pressures. Based on the plasticity index, they concluded that; "*most of surfaces have plasticity indices larger than 1.0, and thus, except for especially smooth surfaces, the asperities will flow plastically under the lightest loads, as has been frequently postulated.*" Chang et al. [43] with the same assumptions as GW, set the criteria for the deformation mode based on the deformation of an average asperity. For compliances less than the critical compliance ω_c, where ω_c is the inception of plastic deformation based on experimental work of Tabor [2] and Johnson [7], the contact is elastic and Hertzian theory can be applied. For compliances higher than ω_c, a plastic model was used. Mikic [45] proposed an alternative plasticity index, $\gamma_{Mikic} = H_{mic}/E'm$. Mikic also reported that the mode of deformation, as stated by GW, depends only on material properties and the shape of the asperities, and it is not sensitive to the pressure level. Mikic performed an analysis to determine the contact pressure over the contact area based on the fact that all contact spots do not have the same contact pressure, although the average contact pressure would remain constant. For surfaces with $\gamma_{Mikic} \geq 3$, 90% of the actual area will have the elastic contact pressure, therefore the contact will be predominantly elastic, and for $\gamma_{Mikic} \leq 0.33$, 90% of the actual area will have the plastic contact pressure, therefore the contact will be predominantly plastic. He concluded that for most engineering surfaces the asperity deformation mode is plastic and the average asperity pressure is the effective microhardness.

To compare elastic and plastic models, Greenwood and Williamson [1] (GW) elastic, Cooper et al. [18] (CMY) plastic, and Tsukizoe and Kisakado [33, 34] (TK) plastic models were chosen, and their trends plotted vs. the dimensionless mean separation. GW requires input surface parameters; η, β and σ, while CMY and TK require σ, m, thus a quantitative comparison between these models requires detailed surface information, and would be restricted to a particular case. However, for a contact, surface parameters are constant and do not change as separation varies. Therefore, by considering surface parameters constant, scale relationships derived and these models compared quantitatively. This comparison only illustrates trend/behavior of surface parameters predicted by each model as the separation changes.

Table 3 shows the scale relationships that were used in the comparison. The real area of microcontacts was calculated from, $A_r = \pi n_s a_s^2$. Additionally, for CMY and TK models, as the fully plastic deformation of asperities was assumed, the external force can be found from, $F = H_{mic}A_r$, where microhardness (for a contact) considered a constant.

The range of separation in typical real contacts is roughly, $1.5 \leq \lambda \leq 3$. The (scale) relationships in Table 3 are plotted versus the separation, λ, over a wider range in Figs. 9 to 12. It can be observed that by decreasing the separation;

- The mean size of microcontacts in all models increases. The size of microcontacts in the TK model increases continuously due to the assumed conical shape of asperities, while the predicted mean microcontact size by GW and CMY approaches some limiting value.
- The real contact area increases and the trends predicted by the three models are very similar, in the applicable range of the separation $1.5 \leq \lambda \leq 3$.
- The external force also increases in a comparable manner in all three models. It is interesting to observe that the external force is (nearly) proportional to the real contact area in GW model, which indicates that GW (elastic) model behaves similar to plastic models and an elastic effective microhardness can be defined.
- The number of microcontacts increases in CMY and TK to a maximum and falls by further decreasing the separation, while the GW model does not show this phenomena. As the separation becomes smaller, more contacting spots form, also the mean size of the existing microcontact increases, until they begin to merge and create larger contact spots (clustering), which results in fewer microcontacts. Based on the microgeometry model, a rough surface can be imagined as a collection of peaks and valleys. At the limit when separation approaches zero, CMY and TK predict that all surface peaks (asperities higher than the mean line) are cut off and only the ones under the mean line (valleys) remain. On the other hand, the GW model predicts that the peaks are elastically compressed to the mean-line,

Table 3. Scale relationships for radius and number of microcontacts, and external force

Model	a'_s	n'_s	F'
GW [1]	$\sqrt{\exp\left(-\lambda^2\right)/\mathrm{erfc}\left(\lambda\right)-\sqrt{\pi}\lambda}$	$\mathrm{erfc}(\lambda)$	$\sqrt{\lambda}\exp\left(-\frac{\lambda^2}{2}\right)\left[\left(1+2\lambda^2\right)K_{\frac{1}{4}}\left(\frac{\lambda^2}{2}\right)-2\lambda^2 K_{\frac{3}{4}}\left(\frac{\lambda^2}{2}\right)\right]$
TK [33, 34]	$1/\lambda$	$\lambda\exp\left(-\lambda^2\right)$	$\exp\left(-\lambda^2\right)/\lambda$
CMY [18]	$\exp\left(\lambda^2\right)\mathrm{erfc}(\lambda)$	$\exp\left(-2\lambda^2\right)/\mathrm{erfc}(\lambda)$	$\mathrm{erfc}(\lambda)$

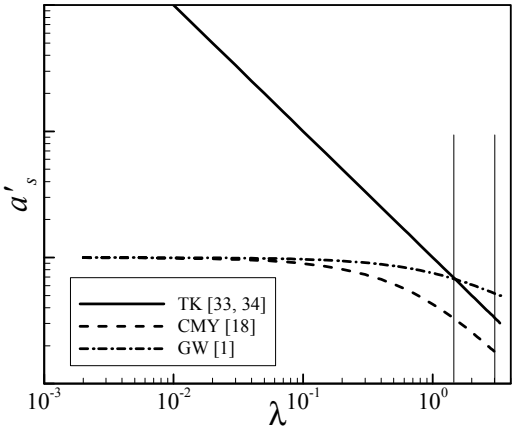

Figure 9. Mean size of microcontacts

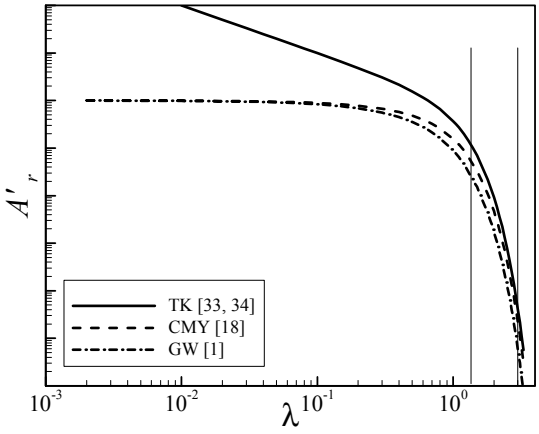

Figure 10. Real contact area

without changing the shape of the rest of the surface profile.

This analysis may not be strictly correct, since these models were not designed to cover a low range of separations and high deformations.

From the comparison, it can be concluded that despite the different basic assumptions and input parameters in the GW elastic and CMY and TK plastic models, their behavior in terms of real contact area, size and number of microcontacts, and the relationship between the external force and real contact area are comparable (in the applicable range of the separation). In a manner similar to Greenwood and Tripp [36] it therefore follows that the behavior of contacting rough surfaces is determined essentially by surface statistical characteristics, which are the same in the compared models, and the deformation mode of asperities is a second order effect. Additionally, a combination of plastic and elastic modes would introduce no new features.

Non-Conforming Rough Surface Models

There are very few analytical models for the contact of non-conforming rough surfaces in the literature. Greenwood and Tripp [36] performed the first in-depth analytical study of the effect of roughness on the pressure distribution and deformation of contacting elastic spherical bodies. The contacting rough surfaces were modeled as a smooth sphere and a rough flat. With the same assumptions as GW, they derived a geometrical relationship relating the local separation to the bulk deformation and the sphere profile. The elastic deformations produced by a normal pressure distribution over an area of the surface can be calculated by superposition, using the Boussinesq solution for a concentrated load on a half-space, and using the fact that the displacement due to an axisymmetric pressure distribution will also be axisymmetric. The most important trends in their model were that an increase in roughness resulted in a decrease in the axial (maximum) contact pressure, P_0, compared with the Hertzian pressure, $P_{0,Hz}$, and enlarges the effective macroscopic contact radius, a_L , beyond the Hertzian contact radius.

Tsukada and Anno [46], with the same assumptions of Greenwood and Tripp [36], developed a model and offered expressions for pressure distribution as a function of $P_0/P_{0,Hz}$ (non-dimensional maximum pressure) and a_L/a_{Hz} (non-dimensional radius of macrocontact area) for

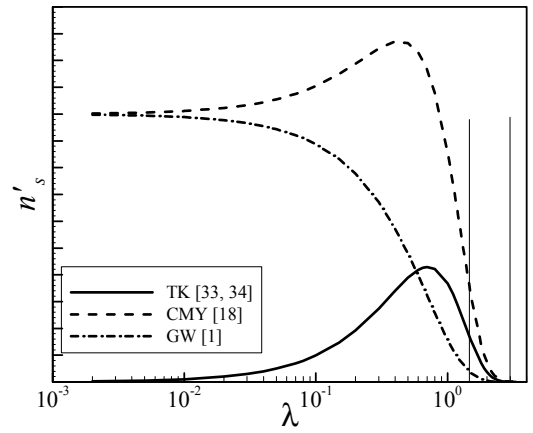

Figure 11. Number of microcontacts

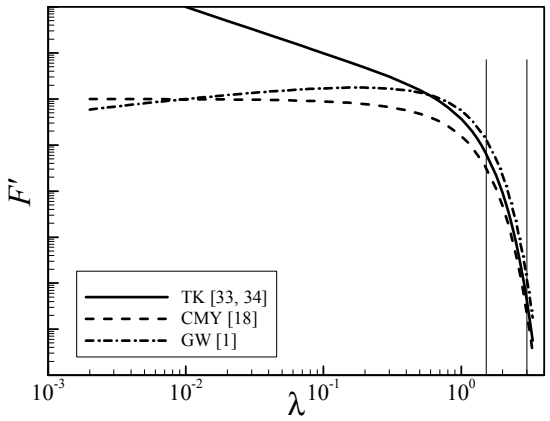

Figure 12. External force

rough sphere-flat contact. Tsukada and Anno [46] and Sasajima and Tsukada [47] presented these two parameters in graphical form for relatively small radii of curvature (5,10, and 15 mm) and roughness in the range of (0.1 to 2 μm) in discrete curves.

THERMAL ANALYSIS

Due to the complex nature of the thermal contact resistance, it is necessary to make some assumptions in order to develop simple thermophysical models. In addition to the geometrical and mechanical assumptions, most existing thermal contact resistance models were based on the following common assumptions:

- contacting solids are isotropic, and thermal conductivity and physical parameters are constant
- contacting solids are thick relative to the roughness or waviness
- surfaces are clean, and contact is static
- radiation heat transfer is negligible
- microcontacts are circular
- steady-state heat transfer at microcontacts
- microcontacts are isothermal; Cooper et al. [18] proved that all microcontacts must be at the same temperature, provided the conductivity in each body is independent of direction, position and temperature
- microcontact spots are flat; it is justifiable by considering the fact that surface asperities usually have a very small slope [4].

Thermal contact models were constructed based on the premise that within the macrocontact area a number of heat channels in the form of cylinders exist. The joint resistance under vacuum conditions can be calculated by superposition of microscopic and macroscopic resistances [3, 4, 5, 48, 21, and 22]:

$$R_j = R_{mic} + R_{mac} \tag{21}$$

The real shapes of microcontacts can be a wide variety of singly connected areas depending on the local profile of the contacting asperities. Yovanovich et al. [49] studied the steady-state thermal constriction resistance of a singly connected planar contact of arbitrary shape. By using an integral formulation and a semi-numerical integration process applicable to any shape, they proposed a definition for thermal constriction resistance based on the square root of the contact area. The square root of the contact area was found to be the characteristic dimension and a non-dimensional constriction resistance based on the square root of area was proposed, which varied by less than 5% for all shapes considered. Therefore, the real shape of the contact spots would be a second order effect, and an equivalent circular contact, which has the same area, can represent contact spots.

Thermal Constriction/Spreading Resistance

The thermal spreading resistance is defined as the difference between the average temperature of the contact area and the average temperature of the heat sink, which is located far from the contact area, divided by the total heat flow rate Q [50, 51]; $R = \Delta T/Q$. Thermal conductance is defined in the same manner as the film coefficient in convective heat transfer; $h = Q/(\Delta T A_a)$.

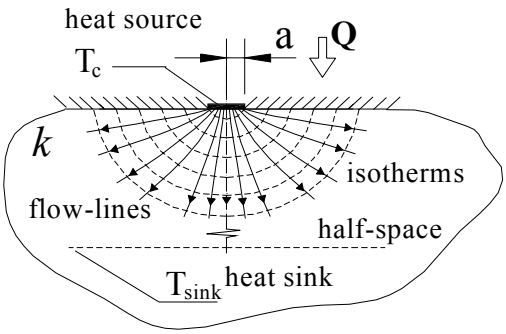

Figure 13. Circular heat source on a half-space

If it is assumed that the micro contacts are very small compared with the distance separating them from each, the heat source on a half-space solution can be used [3]. Figure 13 illustrates geometry of a circular heat source on a half-space. Classical steady-state solutions are available for the circular source areas of radius a on the surface of a half-space of thermal conductivity k, for two boundary conditions; isothermal and isoflux source. The spreading resistance for isothermal and isoflux boundary conditions are $R_{s,isothermal} = 1/(4ka)$, and $R_{s,isoflux} = 8/\left(3\pi^2 ka\right)$, respectively [50]. It can be seen that the difference between the spreading resistance for isoflux and isothermal sources is only 8%, $R_{s,isoflux} = 1.08 R_{s,isothermal}$.

As the microcontacts increase in number and grow in size, a constriction parameter, indicated by $\psi(.)$, must be introduced to account for the interference between neighboring microcontacts. Roess [52] analytically determined the constriction parameter for the heat flow through a flux tube. Figure 14 illustrates the geometry of two flux tubes in a series. An equivalent long cylinder of radius, b, is associated with each microcontact of radius a. The total area of these flux tubes is equal to the interface apparent area. Considering the geometrical symmetry, constriction and spreading resistance are identical and in series, $\psi_{spreading} = \psi_{constriction} = \psi$, Roess [52] suggested an expression in the form of

$$R_{two\ flux\ tubes} = \frac{\psi(\varepsilon)}{4k_1 a} + \frac{\psi(\varepsilon)}{4k_2 a} = \frac{\psi(\varepsilon)}{2k_s a} \qquad (22)$$

where, $k_s = 2k_1 k_2/(k_1 + k_2)$ is the harmonic mean of the thermal conductivities, and $\varepsilon = a/b$. To overcome the mixed boundary value problem, Roess replaced the temperature boundary condition by a heat flux distribution proportional to $\left[1 - (r/a)^2\right]^{-1/2}$ over the source $0 \le r \le a$, and adiabatic outside the source $a < r \le b$. Roess presented his results in the form of a series. Mikic and Rohsenow [4], by using a superposition method, derived an expression for the thermal contact resistance for half of an elemental heat channel (semi-infinite cylinder), with isothermal boundary condition. They found another solution for mixed boundary condition of the flux tube, by using a procedure similar to Roess [52]. They also studied thermal contact resistance of the flux tube with a finite length. It was shown that the influence of the finite length of the elemental heat channel on the contact resistance was negligible for all values of $l \ge b$, where l is the length of the flux tube. Later this expression was simplified by Cooper et al. [18], see Table 4. Yovanovich [51] generalized the solution to include the case of uniform heat flux, and arbitrary heat flux over the microcontact. A number of correlations for isothermal spreading resistance for the flux tube are listed in Table 4. Figure 15 shows the comparison between these correlations. It is observed that at the limit when $\varepsilon \to 0$, the flux tube spreading resistance factor approaches one, which is the case of a heat source on a half-space. Also the results from all these various correlations for spreading resistance factor show very good agreement for the range $0 \le \varepsilon \le 0.3$, which is typically the range of interest in thermal contact resistance applications.

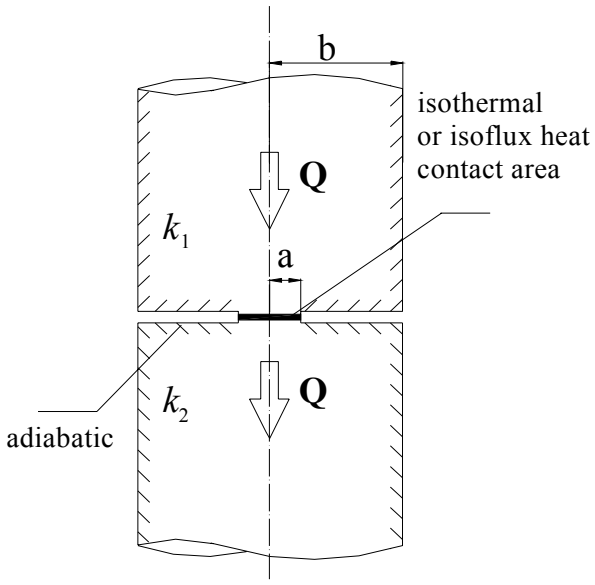

Figure 14. Two flux tubes in series

Table 4. Thermal spreading resistance factor correlations, isothermal contact area

Reference	Correlation
Roess [52]	$1-1.4093\varepsilon+0.2959\varepsilon^3+0.0525\varepsilon^5$ $+0.021041\varepsilon^7+0.0111\varepsilon^9+0.0063\varepsilon^{11}$
Mikic-Rohsenow [4]	$1-4\varepsilon/\pi$
Cooper et al. [18]	$(1-\varepsilon)^{1.5}$
Gibson [61]	$1-1.4092\varepsilon+0.3381\varepsilon^3+0.0679\varepsilon^5$
Negus-Yovanovich [62]	$1-1.4098\varepsilon+0.3441\varepsilon^3+0.0431\varepsilon^5$ $+0.0227\varepsilon^7$

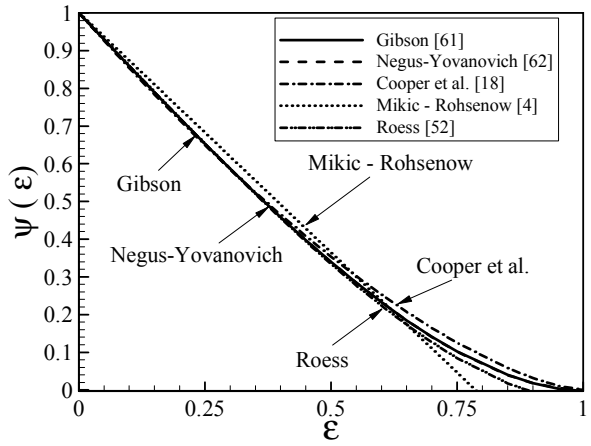

Figure 15. Comparison between thermal spreading resistance correlations, isothermal contact area

TCR Models for Conforming Rough Surfaces

During the last four decades, a number of experimental works have been done and a number of correlations were proposed for nominally flat rough surfaces. Madhusudana and Fletcher [6], and Sridhar and Yovanovich [53] reviewed existing conforming rough models. Here only a few models will be reviewed, in particular those that are going to be compared with experimental data.

Cooper et al. [18] developed an analytical model, with the same assumptions that were discussed at the beginning of this section, for contact of flat rough surfaces in a vacuum. Eq.(15) shows the mean size and number of microcontacts and Eq.(16) presents the ratio of real area to the apparent area. The remaining relations of the Cooper et al. [18] model is

$$R_c=\frac{4\sqrt{\pi}}{A_a\sqrt{2}k_s}\left(\frac{\sigma}{m}\right)\frac{\left[1-\sqrt{\frac{1}{2}\mathrm{erfc}\left(\lambda\right)}\right]^{1.5}}{\exp\left(-\lambda^2\right)} \tag{23}$$

where, R_c, λ $=\mathrm{erfc}^{-1}\left(2P_m/H_{mic}\right)$, and k_s are thermal contact resistance, dimensionless separation, and harmonic mean of thermal conductivities, respectively. Yovanovich [54] suggested a correlation based on the Cooper et al. [18] model, which is quite accurate for optically flat surfaces

$$R_c=\frac{(\sigma/m)}{1.25A_ak_s\left(P/H_c\right)^{0.95}} \tag{24}$$

TCR Models for Non-Conforming Rough Surfaces

Clausing and Chao [3] were the first to experimentally study the contact of rough non-flat surfaces. They also developed an analytical model, with the same assumptions that were discussed at the beginning of this section, for determining the thermal joint (macroscopic and microscopic) resistance for rough, spherical surfaces in contact under vacuum conditions. Their geometrical contact model is shown in Fig.16, the effective radius of curvature of the contacting surface was found from Eq.(8). Using Roess [52] correlation (see Table 4), the total micro thermal resistance of identical, circular, isothermal contact spots in the macrocontact area was

$$R_s=\frac{\psi\left(\varepsilon_s\right)}{2k_sa_sn_s} \tag{25}$$

The microscopic portion of the Clausing and Chao [3] model was based on the plastic deformation of asperities; a measured diamond pyramid hardness was used to consider the asperity hardness of the contacting surfaces. However, material microhardness was multiplied by, ξ, an empirical correction factor introduced by Holm [31], to account for the effects of elastic deformation of asperities. The real contact area A_r, then was calculated

$$A_r=\frac{F}{\xi H_{mic}}=n_s\pi a_s^2 \tag{26}$$

Additionally the following simplifications were made to enable an estimation of the microscopic constriction resistance:

- the microscopic contact spots were assumed to be identical and uniformly distributed, in a triangular array, over the macrocontact area, see Fig.16

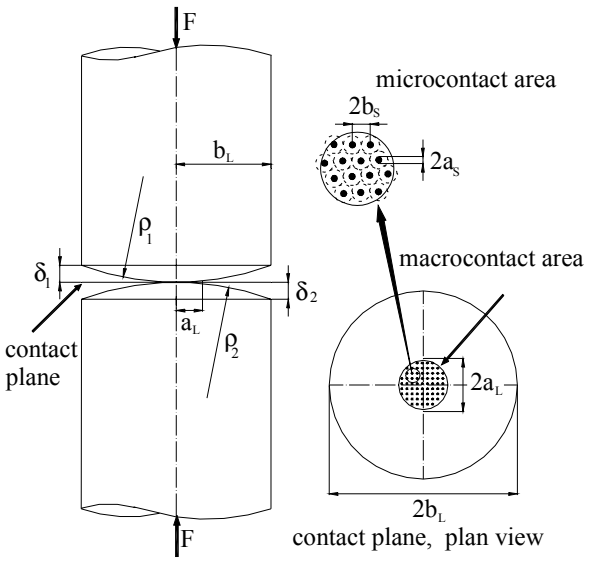

Figure 16. Clausing and Chao [3, 20] geometrical model

- the average size of the microcontacts a_s was independent of load and it was of the same order of magnitude as the surface roughness, i.e. $a_s \equiv \sigma$.

They did not report the exact relationship between the microcontact spot size and the roughness. In this study, it is assumed, $a_s = \sigma$. They assumed an average value of $\xi = 0.3$ to take into account both plastic and elastic deformation of microcontacts. Also, a value of $\psi(\varepsilon_s) = 1$ was assumed, which means microcontacts were considered as isothermal circular heat sources on a half-space [3], additionally they assumed, $\xi\pi = 1$. With the above assumptions the microscopic thermal resistance became:

$$R_s = \frac{\sigma H_{mic}}{2k_s F} \tag{27}$$

Neglecting the effect of roughness on the macrocontact area, the radius of macrocontact, a_L, was obtained from the Hertz theory, Eq.(13), for elastic contact of spheres, reported in the form (assuming Poisson's ratio $\upsilon_1^2 = \upsilon_2^2 = 0.1$)

$$\varepsilon_L = \frac{a_{Hz}}{b_L} = 1.285 \left[\left(\frac{P}{E_m} \right) \left(\frac{b_L}{\delta} \right) \right]^{1/3} \tag{28}$$

where, $E_m = 2E_1E_2/(E_1 + E_2)$, and $\delta = \delta_1 + \delta_2$. Therefore, the thermal joint resistance, based on the Clausing and Chao [3] model, became

$$R_j = \frac{\sigma H_{mic}}{2k_s F} + \frac{\psi(\varepsilon_L)}{2k_s a_L} \tag{29}$$

where, $\psi(.)$ is the Roess [52] spreading factor (see Table 4). Clausing and Chao [3] verified their model against experimental data and showed good agreement. Their model was suitable for situations in which the macroscopic constriction resistance was much greater than the microscopic resistance.

Kitscha [55] and Fisher [56] developed models similar to Clausing and Chao's [3] model and experimentally verified their models for relatively small radii of curvature and different levels of roughness. Burde [48] derived expressions for size distribution, and number of microcontacts, which described the increase in the macroscopic contact radius for increasing roughness. His model showed good agreement with experimental data for spherical specimens with relatively small radii of curvature with different levels of roughness. Burde did not verify his model or perform experiments for surfaces approaching nominally flat. Also, results of his model were reported in the form of many plots, which are not convenient to use.

Mikic and Rohsenow [4] studied thermal contact resistance for various types of surface waviness and conditions. In particular; nominally flat rough surface in a vacuum, nominally flat rough surfaces in a fluid environment, smooth wavy surfaces in a vacuum environment (with either of the following three types of waviness involved: spherical, cylindrical in one direction, and cylindrical in two perpendicular direction), and rough spherical wavy surfaces in a vacuum. Thermal contact resistance for two spherical wavy rough surfaces was considered as the summation of a micro and a macro thermal constriction resistance given by

$$R_j = \frac{\psi(a_{L,\text{eff}}/b_L)}{2k_s a_{L,\text{eff}}} + \frac{\psi(\varepsilon_s)}{2k_s a_s n_s} \tag{30}$$

where, $\psi(.)$ is the Mikic and Rohsenow [4] spreading factor (see Table 4). Similar to Clausing and Chao [3], the effective radius of curvature of the contacting surface was found from Eq.(8). The macrocontact area (for smooth surfaces) was determined by the Hertzian theory, Eq.(13). Mikic and Rohsenow [4], assuming fully plastic deformation of asperities and equivalent surface approximation, derived expressions for the mean size and number of microcontacts that were used later by Cooper et al. [18]. Their model was based on the uniform distribution of identical microcontacts inside the macrocontact area. In case of rough

surface contacts, knowing that the macrocontact area would be larger than the one predicted by Hertz theory, they defined an effective macrocontact area. This area contained all the microcontact spots as if they had been uniformly distributed. Using this definition and the assumption that the mean surface would deform elastically, they suggested an iterative procedure for calculating the macrocontact radius. Mikic and Rohsenow verified their model against three experiments. Their computed ratios of macrocontact radius to Hertzian macrocontact radius were 1.6, 1.6, and 1.77 for each experiment and were considered constant throughout the tests, as the external load increased. Mikic and Rohsenow did not derive the actual continuously varying pressure distribution for the contact of spherical rough surfaces. Additionally their expressions for effective macrocontact radius were very complex, and the iterative solution was quite tedious.

Later Mikic [57] derived expressions, based on the Mikic and Rohsenow [4] plastic model, for macroscopic and microscopic thermal resistances in a vacuum, which related thermal resistances (micro and macro) to arbitrary pressure distribution and surface properties. The derived relations were general in the sense that they did not require the knowledge of the effective macrocontact area and they could be applied for any symmetrical cylindrical or Cartesian pressure distribution at an interface.

Lambert [13] studied the thermal contact resistance of two rough spheres in a vacuum. He started with the Greenwood and Tripp [36] elastic model for mechanical analysis, and Mikic [57] thermal model as the basis for his thermal analysis. Lambert [13] was not able to solve the set of the mechanical relationships numerically, and mentioned that "*the Greenwood and Tripp [13] model is under-constrained, and convergence may be achieved for the physically impossible cases*". To obtain numerical convergence, Lambert implemented results for the dimensionless axial minimum mean plane, reported by Tsukada and Anno [46], in the mechanical part of his model. The procedure for applying the Lambert [13] model (presented in appendix-A of his thesis) was used to calculate thermal contact resistance in this study. He suggested two 7th order polynomial expressions for pressure distribution and radius of macrocontact area as a function of dimensionless load. Lambert also introduced three dimensionless correction functions in the form of logarithmic polynomials in his thermal model, without specifying the origin and reasons for their presence. His approximate procedure was quite long and required computer-programming skills to apply it. Also, logarithmic expressions for dimensionless macrocontact radius, a_L/a_{Hz} , showed a discontinuity, which caused a strange behavior in predicted thermal joint resistance (see Figs.17 and 18). Lambert collected and summarized experimental data reported by many researchers and compared his model with experimental data. He showed a good agreement with experimental data for nominally flat rough surfaces.

Table 5. Parameter ranges for experimental data

Parameters
$57.3 \leq E' \leq 114.0\ (GPa)$
$16.6 \leq k_s \leq 75.8\ (W/mK)$
$0.12 \leq \sigma \leq 13.94\ (\mu m)$
$0.04 \leq m \leq 0.34\ (-)$
$0.013 \leq \rho \lessapprox 120\ (m)$

Nishino et al. [21] studied the contact resistance of spherical rough surfaces in a vacuum under low applied load. Macroscopic and microscopic thermal contact resistance was calculated based on the Mikic [57] thermal model. Nishino et al. [21] used a pressure measuring colored film that provided information, by means of digital image processing, about the contact pressure distribution. They also verified their method experimentally with aluminum alloy specimens, the experimental data showed good agreement with their technique. They concluded that the macroscopic constriction resistance was predominant under the condition of low applied load. However, the Nishino et al. model required measurements with pressure sensitive film and they did not suggest a general relationship between contact pressure and surface profile and characteristics.

COMPARISON BETWEEN TCR MODELS AND EXPERIMENTAL DATA

The developed theoretical models by Clausing and Chao [3] Eq.(29), Yovanovich [54] Eq.(24), and Lambert [13] are compared with experimental data. References, material and physical properties, and surface characteristics of the experimental data are summarized in Table 5. As indicated in Table 5, the experimental data cover a relatively wide range of the experimental parameters.

The comparison is done at two extremes; conforming rough surfaces, where the macro resistance is negligible, and elasto-constriction limit, where contacting surfaces have relatively small radii of curvature and the micro resistance is almost negligible.

Thermal contact resistance for the above models was calculated for a base typical rough surface, the physical properties and surface characteristics are shown in Table 6. $\rho = 14.3\,(mm)$, and $\rho = 100\,(m)$ for elasto-constriction and conforming rough limits, respectively. Experimental data collected by Kitscha [55], Fisher [56], and

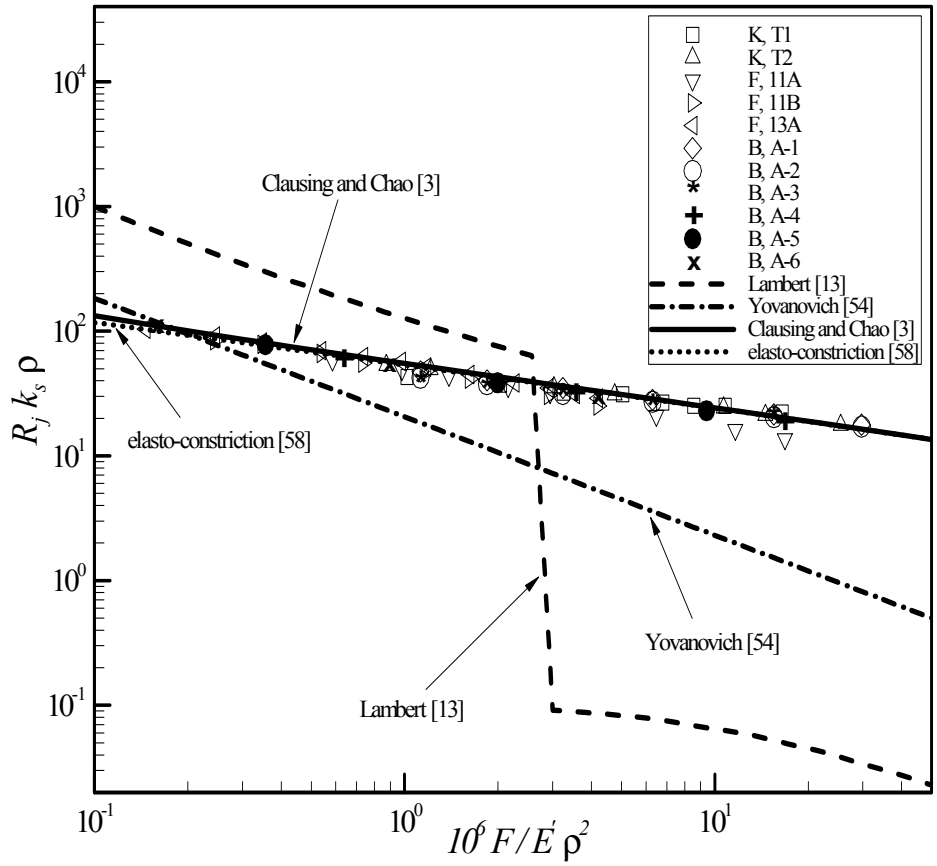

Figure 17. Comparison of models with data at the elasto-constriction limit

Table 6. Physical properties and surface characteristics of comparison base surface

$\sigma = 1.3\,(\mu m)$	$m = 0.073$	$H_{mic} = 3.92(GPa)$
$b_L = 7.15\,(mm)$	$E' = 114(GPa)$	$k_s = 40.7\,(W/mK)$

Burde [48] were compared with the theoretical models in Fig.17. The elasto-constriction approximation introduced by Yovanovich [58], which accounts only for macro resistance predicted by Hertz theory and neglects the micro thermal resistance completely, was also included in the comparison. The elasto-constriction approximation was included to clearly demonstrate that the macro resistance is the dominating part of thermal joint resistance in the elasto-constriction limit, and the micro thermal resistance is negligible. As can be seen in Fig.17, the elasto-constriction approximation and the Clausing and Chao [3] model are very close and show good agreement with the data. The Lambert [13] model, as the result of its expression for macro-contact radius a_L, showed a strange behavior. As expected, Yovanovich [54] model, which was developed for conforming rough surfaces, does not agree with the data.

Experimental data collected by Antonetti [59], Hegazy [24], and Milanez et al. [60] were compared with the theoretical models in Fig.18. As shown, the Yovanovich [54] model showed good agreement with the data. Lambert [13] was very close to Yovanovich [54] in most of the comparison range, however the strange behavior in the predicted macrocontact area showed up as can be seen in the plot. The Clausing and Chao [3] model under predicted thermal resistance in the conforming rough region.

Kitscha [55], and Fisher [56] did not report the surface slope, m; the Lambert [13] correlation was used to estimate these values (see Table 1). The exact values of radii of curvature for conforming rough surfaces were not reported. Since, these surfaces were prepared to be optically flat, radii of curvature in the order of $\rho \approx 100\,(m)$ are considered for these surfaces. Table 9 indicates the researchers and the specimen materials used in the experiments.

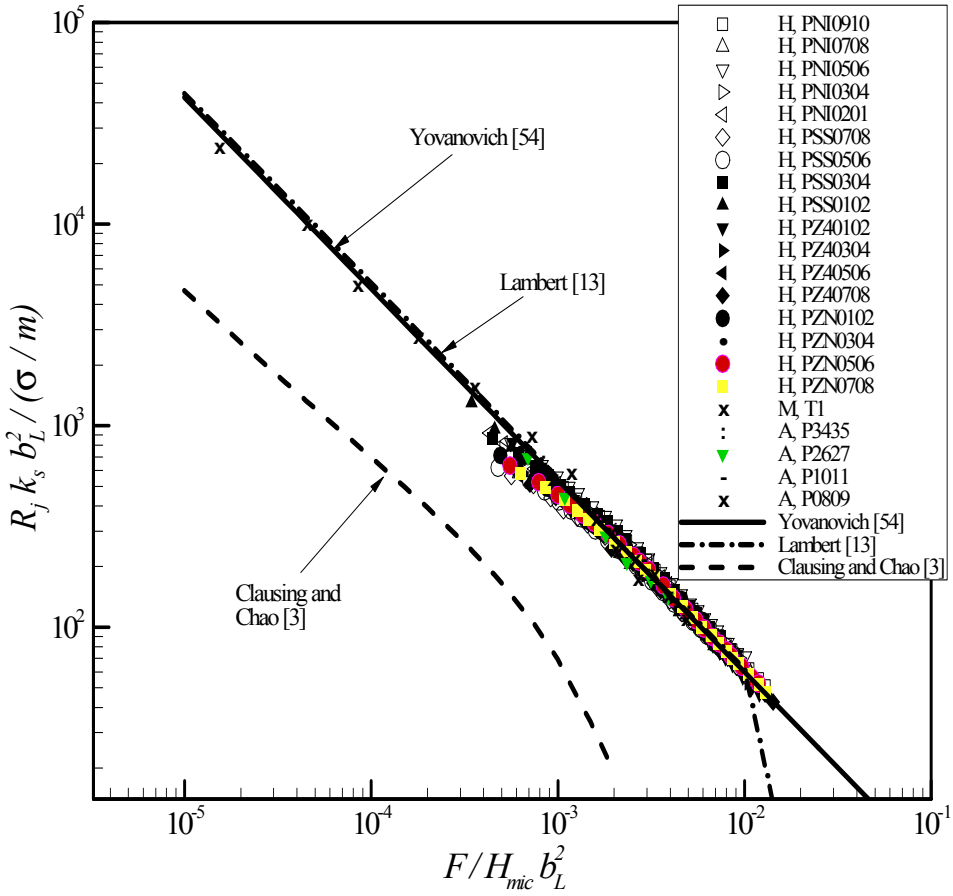

Figure 18. Comparison of models with data at the conforming rough limit

CONCLUDING REMARKS

Thermal contact resistance modeling and its components are studied. The modeling process is divided into three analyses: geometrical, mechanical, and thermal. Also each one includes a macro and micro scale part.

Suggested empirical correlations to relate surface slopes, m, to surface roughness, are summarized and compared with experimental data. The comparison shows that the uncertainty of the correlations is high, and use of these correlations is not recommended unless only an estimation of m is required.

GW[1] elastic, CMY [18] and TK [33, 34] plastic conforming rough models are reviewed, and a set of scale relationships for the contact parameters, i.e. the mean microcontact size, number of microcontacts, density of microcontacts, and the external load as functions of dimensionless separation are derived. These scale relationships are compared and it is graphically shown that despite the different assumptions and input parameters, their behaviors in terms of the contact parameters are similar. It can be concluded from the comparison that the behavior of contacting rough surfaces is determined essentially by surface statistical characteristics. Also a combination of plastic and elastic modes would introduce no new features.

The common assumptions of the existing thermal analyses are summarized. Suggested correlations by different researchers for the flux tube spreading resistance are compared. It was observed that, at the limit, the correlations approach the case of a heat source on a half-space. Also all the spreading resistance correlations show good agreement for the applicable range.

Experimental data points obtained for five materials, namely SS 304, carbon steel, nickel 200, zirconium-2.5% niobium, and Zircaloy-4, are summarized and grouped into two limiting cases: conforming rough, and elasto-constriction. These data are non-dimensionalized and compared with TCR models at the two limiting cases. It is observed that none of the existing theoretical models covers both of the above-mentioned limiting cases. This clearly shows the need to develop theoretical model(s) which can predict TCR

Table 7. Summary of physical properties and surface charactersitics, conforming rough limit

Ref.	E'	σ	m	c_1	-c_2	k_s	b_L
A,P3435	112.1	8.48	.34	6.3	.26	67.1	14.3
A,P2627	112.1	1.23	.14	6.3	.26	64.5	14.3
A,P1011	112.1	4.27	.24	6.3	.26	67.7	14.3
A,P0809	112.1	4.29	.24	6.3	.26	67.2	14.3
H,NI12	112.1	3.43	.11	6.3	.26	75.3	12.5
H,NI34	112.1	4.24	.19	6.3	.26	76.0	12.5
H,NI56	112.1	9.53	.19	6.3	.26	75.9	12.5
H,NI78	112.1	13.9	.23	6.3	.26	75.7	12.5
H,NI910	112.1	0.48	.23	6.3	.26	75.8	12.5
H,SS12	112.1	2.71	.07	6.3	.23	19.2	12.5
H,SS34	112.1	5.88	.12	6.3	.23	19.1	12.5
H,SS56	112.1	10.9	.15	6.3	.23	18.9	12.5
H,SS78	112.1	0.61	.19	6.3	.23	18.9	12.5
H,Z412	57.3	2.75	.05	3.3	.15	16.6	12.5
H,Z434	57.3	3.14	.15	3.3	.15	17.5	12.5
H,Z456	57.3	7.92	.13	3.3	.15	18.6	12.5
H,Z478	57.3	0.92	.21	3.3	.15	18.6	12.5
H,ZN12	57.3	2.50	.08	5.9	.27	21.3	12.5
H,ZN34	57.3	5.99	.16	5.9	.27	21.2	12.5
H,ZN56	57.3	5.99	.18	5.9	.27	21.2	12.5
H,ZN78	57.3	8.81	.20	5.9	.27	21.2	12.5
M,SS1	113.8	0.72	.04	6.3	.23	18.8	12.5

Table 8. Summary of the physical properties and surface characteristics, elasto-constriction limit

Ref.	E'	σ	m	ρ	c_1	c_2	k_s	b_L
B, A-1	114.0	0.63	.04	.0143	3.9	0	40.7	7.2
B, A-2	114.0	1.31	.07	.0143	3.9	0	40.7	7.2
B, A-3	114.0	2.44	.22	.0143	3.9	0	40.7	7.2
B, A-4	114.0	2.56	.08	.0191	4.4	0	40.7	7.2
B, A-5	114.0	2.59	.10	.0254	4.4	0	40.7	7.2
B, A-6	114.0	2.58	.10	.0381	4.4	0	40.7	7.2
F, 11A	113.1	0.12	-	.0191	4.0	0	57.9	12.5
F, 11B	113.1	0.12	-	.0381	4.0	0	57.9	12.5
F, 13A	113.1	0.06	-	.0381	4.0	0	58.1	12.5
K, T1	113.8	0.76	-	.0135	4.0	0	51.4	12.7
K, T2	113.8	0.13	-	.0135	4.0	0	51.4	12.7

Table 9. Reseacher and specimen materials

Ref.	Researcher	Specimen Material(s)
A	Antonetti [59]	Ni 200
B	Burde [48]	SPS 245, Carbon Steel
F	Fisher [56]	Ni 200, Carbon Steel
H	Hegazy [24]	Ni 200
		SS 304
		Zircaloy4
		Zr-2.5%wt Nb
K	Kitscha [55]	Steel 1020,Carbon Steel
M	Milanez et al. [60]	SS 304

over all cases including the above mentioned limiting cases and the transition range where both roughness and out-of-flatness are present and their effects on contact resistance are of the same order.

ACKNOWLEDGMENT

The authors gratefully acknowledge the financial support of the Centre for Microelectroncis Assembly and Packaging, CMAP and the Natural Sciences and Engineering Research Council of Canada, NSERC.

REFERENCES

[1] Greenwood, J. A. and Williamson, B. P., 1966, "Contact of Nominally Flat Surfaces," Proc., Roy. Soc., London A295, pp. 300-319.
[2] Tabor, D., 1952, *The Hardness of Metals*, Oxford, London.
[3] Clausing, A. M. and Chao, B.T., 1963, "Thermal Contact Resistance in a Vacuum Environment," University of Illinois, Urbana, Illinois, Report ME-TN-242-1, August.
[4] Mikic, B. B., Rohsenow, W. M., 1966, "Thermal Contact Conductance," Technical Report No. 4542-41, Dept. of Mech. Eng. MIT, Cambridge, Massachusetts, NASA Contract No. NGR 22-009-065, September.
[5] Yovanovich, M. M., 1969, "Overall Constriction Resistance Between Contacting Rough, Wavy Surfaces," Int. J. Heat Mass Transfer 12, pp. 1517-1520.
[6] Madhusudana, C. V. and Fletcher, L. S., 1981, "Ther-

mal Contact Conductance: A Review of Recent Literature," Mech. Eng. Dept. Texas A&M University, September.
[7] Johnson, K. L., 1985, *Contact Mechanics*, Cambridge University Press, Cambridge.
[8] Liu, G., Wang, Q. and Lin, C., 1999, "A Survey of Current Models for Simulating the Contact Between Rough Surfaces," Tribology Trans., Vol. 42, 3, pp. 581-591.
[9] ANSI B46.1-1985, American National Standards Institute / American Society of Mechanical Engineers, 1985, Surface Texture: Surface Roughness, Waviness and Lay, March.
[10] Ling, F. F., 1958, "On Asperity Distributions of Metallic Surfaces," Journal of Applied Physics, Vol. 29, No.8.
[11] Tanner, L. H. and Fahoum, M., 1976, "A Study of The Surface Parameters of Ground and Lapped Metal Surfaces, Using Specular and Diffuse Reflection of Laser Light," Wear, 36, pp. 299-316.
[12] Antonetti, V. W., Whittle, T. D. and Simons, R. E., 1991, "An Approximate Thermal Contact Conductance Correlation," ASME, The 28th National Heat Transfer Conference Minneapolis, Minnesota, HTD-Vol. 170, Experimental/ Numerical Heat Transfer in Combustion and Phase Change, pp. 35-42.
[13] Lambert, M. A., 1995, "Thermal Contact Conductance of Spherical, Rough Metals," Ph.D. Thesis, Dept. of Mech. Eng., Texas A&M University, USA.
[14] Francois, R. V., 2001, "Statistical Analysis of Asperities on a Rough Surface," Wear 249, pp. 401-408.
[15] Williamson, J. B. P., Pullen, J. and Hunt, R. T., 1969, "The Shape of Solid Surfaces," Surface Mechanics, ASME, New York, pp. 24-35.
[16] Greenwood, J. A., 1967, "The Area of Contact Between Rough Surfaces and Flats," Journal of Lubrication Tech., Jan. 1967, pp. 81- 91
[17] Bendat, J. S., 1958, *Principal and Applications of Random Noise Theory*, Wiley, New York.
[18] Cooper, M. G., Mikic, B .B. and Yovanovich, M. M., 1969, "Thermal Contact Conductance," Int. J. Heat Mass Transfer, Vol.12, pp. 279-300.
[19] Francis, H. A., 1977, "Application of Spherical Indentation Mechanics To Reversible and Irreversible Contact Between Rough Surfaces," Wear, 45, pp. 221-269.
[20] Clausing, A. M. and Chao, B. T., 1965, "Thermal Contact Resistance in a Vacuum Environment," Paper No.64-HT-16, Transactions of ASME: Journal of Heat Transfer, Vol. 87, Nov. pp. 243-251.
[21] Nishino, K., Yamashita, S. and Torii, K., 1995, "Thermal Contact Conductance Under Low Applied Load in a Vacuum Environment," Experimental Thermal and Fluid Science, Elsevier, New York, 10, pp. 258-271.
[22] Lambert, M. A. and Fletcher, L. S., (1997), "Thermal Contact Conductance of Spherical Rough Metals," Transactions of ASME, Vol.119, Nov., pp. 684-690.
[23] Mott, M. A., 1956, *Micro-Indentation Hardness Testing*, Butterworths Scientific Publications, London.
[24] Hegazy, A. A., 1985, "Thermal Joint Conductance of Conforming Rough Surfaces: Effect of Surface Micro-Hardness Variation," Ph.D. Thesis, Dept. of Mech. Eng., University of Waterloo, Waterloo, Canada.
[25] Song, S. and Yovanovich, M. M., 1988, "Relative Contact Pressure: Dependence on Surface Roughness and Vickers Microhardness," AIAA Journal of Thermophysics and Heat Transfer, Vol. 2, No. 1, pp. 43-47.
[26] Sridhar, M. R., 1994, "Elastoplastic Contact Models For Sphere-Flat and Conforming Rough Surface Applications," Ph.D. Thesis, Dept. of Mech. Eng., University of Waterloo, Waterloo, Canada.
[27] Hertz, H., 1881, "On the Contact of Elastic Bodies," Journal fur die reine und angewandie Mathematic, Vol. 92,p. 156-171 (In German).
[28] Hardy, C., Baronet, C. N. and Tordion, G. V., 1971, "Elastoplastic Indentation of a Half-space by a Rigid Sphere," Journal of Numerical Methods in Engineering, 3, 451.
[29] Abott, E. J. and Firestone, F. A., 1933, "Specifying Surface Quality," Mechanical Engineering (ASME), 55, 569.
[30] Bowden, F. P. and Tabor, D., 1951, *Friction and Lubrication of Solids*, Oxford University Press, UK.
[31] Holm, R., 1958, *Electrical Contacts 3rd Ed*, Springer Verlag, Berlin.
[32] Pullen, J. and Williamson, J. B. P., 1972, "On the Plastic Contact of Rough Surfaces," Roy. Soc. London A.327, 159-173.
[33] Tsukizoe, T. and Hisakado, T., 1965, "On the Mechanism of Contact Between Metal Surfaces- The Penetrating Depth and the Average Clearance," Journal of Basic Eng., Vol. 87, No. 3, pp. 666-674.
[34] Tsukizoe, T. and Hisakado, T., 1968, "On the Mechanism of Contact Between Metal Surfaces: Part 2- The Real Area and the Number of the Contact Points," Journal of Lubrication Tech., Vol. 40, No.1, pp. 81-88.
[35] Archard, J. F., 1953, "Contact and Rubbing of Flat Surfaces," Journal of Applied Physics, Vol. 24, pp. 981.
[36] Greenwood, J. A. and Tripp, J. H., 1967, "The Elastic Contact of Rough Spheres," Transactions of the ASME: Journal of Applied Mechanics, Vol. 89, No.1, pp. 153-159.
[37] Whitehouse, D. J. and Archard, J. F., 1970, "The Properties of Random Surfaces of Significance in Their Contact," Proc. Roy. Soc. London, A316, 97-121.
[38] Bush, A. W., Gibson, R. D. and Keogh, G. P., 1979, "Strongly Anistropic Rough Surfaces," ASME Journal of Lubrication Tech., Vol. 101, pp. 15-20.

[39] Onions, R. A. and Archard, J. F., 1973, "The Contact of Surfaces Having a Random Structure," Journal of Physics D., 6, pp. 289-304.
[40] Bush, A.W., Gibson, R. D. and Thomas, T. R., 1975, "The Elastic Contact of a Rough Surface," Wear, 35, pp. 87-111.
[41] O'Callaghan, M. and Cameron, M. A., 1976, "Static Contact Under Load Between Nominal Flat Surfaces in Which Deformation Is Purely Elastic," Wear, Vol. 36, pp.79-97.
[42] McCool, J. I., 1986, "Comparison of Models for the Contact of Rough Surfaces," Wear, Vol. 107, pp. 37-60.
[43] Chang, W. R., Etsion, I. and Bogy, D. B., 1987, "An Elastic-Plastic Model for the Contact of Rough Surfaces," J. Tribology, Vol. 109, pp. 257-253.
[44] Zhao, Y., Maietta, D.M. and Chang, L., 2000, "An Asperity Microcontact Model Incorporating the Transition From Elastic Deformation to Fully Plastic Flow" Trans. of ASME, Vol.122, Jan. 2000, pp. 86-93.
[45] Mikic, B. B., 1974, "Thermal Contact Conductance: Theoretical Considerations," Int. J. of Heat and Mass Transfer, Vol. 17, 205.
[46] Tsukada, T. and Anno, Y., 1979, "On the Approach Between a Sphere and a Rough Surface (1st. Report-Analysis of Contact Radius and Interface Pressure," (in Japanese), Journal of the Japanese Society of Precision Engineering, Vol. 45, No. 4, pp. 473-479.
[47] Sasajima, K. and Tsukada, T., 1981, "On the Approach Between a Sphere and a Rough Surface (2nd. Report- Critical Condition to Yield Plastic Deformation in Contacting Bodies," (in Japanese), Journal of the Japanese Society of Precision Engineering, Vol. 47, No. 6, pp. 694-699.
[48] Burde, S. S., 1977, "Thermal Contact Resistance Between Smooth Spheres and Rough Flats," Ph.D. Thesis, Dept. of Mech. Eng., University of Waterloo, Waterloo, Canada.
[49] Yovanovich M. M., Burde, S. S. and Thompson, C. C., 1976, "Thermal Constriction Resistance of Arbitrary Planar Contacts With Constant Flux," presented at AIAA 11th Thermophysics Conference, San Diego, California, July 14-16, Paper No. 76-440, pp. 127-139.
[50] Carslaw, H. S. and Jaeger, J. C., 1959, Conduction of Heat in Solids, 2nd Edition. Oxford Press., London.
[51] Yovanovich, M. M., 1976, "Thermal Constriction Resistance of Contacts on a Half-Space: Integral Formulation," AIAA Progress in Astronautics and Aeronautics, Radiative Transfer and Thermal Control, Vol. 49, AIAA NY, pp. 397-418.
[52] Roess, L. C., 1950, "Theory of Spreading Conductance," Beacon Laboratories of Texas, Beacon, NY, Appendix A (Unpublished paper).
[53] Sridhar, M. and Yovanovich, M. M., 1993, "Critical Review of Elastic and Plastic Thermal Conductance Models and Comparison With Experiment," Paper No. AIAA 93-2776, presented at the AIAA 28th Thermophysics Conference, Orlando, Florida, July 6-9.
[54] Yovanovich, M. M., 1982, "Thermal Contact Correlations," in Horton, T.E. (editor), Progress in Aeronautics and Aerodynamics: Spacecraft Radiative Transfer and Temperature Control, Vol. 83, pp. 83-95.
[55] Kitscha, W., 1982, "Thermal Resistance of the Sphere-Flat Contact," M.A.Sc. Thesis, Dept. of Mech. Eng., University of Waterloo, Waterloo, Canada.
[56] Fisher, N. J., 1985, "Analytical and Experimental Studies of the Thermal Contact Resistance of Sphere/Layered Flat Contacts," M.A.Sc. Thesis, Dept. of Mech. Eng., University of Waterloo, Waterloo, Canada.
[57] Mikic, B. B., 1970, "Thermal Constriction Resistance Due to Non-Uniform Surface Conditions; Contact Resistance at Non-Uniform Interface Pressure," Int. J. of Heat and Mass Transfer, Vol.13, pp. 1497-1500.
[58] Yovanovich, M. M., 1986, "Recent Developments In Thermal Contact, Gap and Joint Conductance Theories and Experiment," Delivered at the Eight International Heat Transfer Conference, San Francisco, CA, August 17-22, pp. 35-45.
[59] Antonetti, V. W., 1983, "On the Use of Metallic Coating to Enhance Thermal Contact Conductance," Ph.D. Thesis, Dept. of Mech. Eng., University of Waterloo, Waterloo, Canada.
[60] Milanez, F. H., Yovanovich, M. M., and Mantelli, M. B. H., 2003, "Thermal Contact Conductance at Low Contact Pressures," to be presented at the 36th AIAA Thermophysics Conference, June 23-26, Orlando, FL.
[61] Gibson, R. D., 1976, "The Contact Resistance of a Semi-Infinite Cylinder in a Vacuum," Applied Energy, Vol.2, pp. 57-65.
[62] Negus, K. J. and Yovanovich, M. M., 1984, "Application of the Method of Optimized Images to the Steady Three Dimensional Conduction Problems," ASME 84-WA/HT-110.
[63] McMillan, R. Jr. and Mikic, B. B., 1970, "Thermal Contact Resistance With Non-Uniform Interface Pressures," Technical Report No. DSR 72105-70, Dept. Of Mech. Eng. MIT, Cambridge, Massachusetts, NASA Contract No. NGR 22-009-(477), November.